

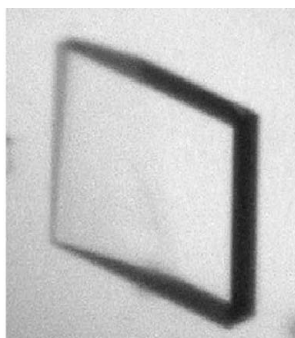
Inmaculada Gómez García,^a
Caren L. Freel Meyers,^{b,‡}
Christopher T. Walsh^b and
David M. Lawson^{a*}

^aDepartment of Biological Chemistry, John Innes Centre, Norwich NR4 7UH, England, and
^bDepartment of Biological Chemistry and Molecular Pharmacology, Harvard Medical School, Boston, MA 02115, USA

‡ Present address: Department of Pharmacology and Molecular Sciences, Johns Hopkins University School of Medicine, Baltimore, MD 21205, USA.

Correspondence e-mail:
david.lawson@bbsrc.ac.uk

Received 2 September 2008
Accepted 18 September 2008



© 2008 International Union of Crystallography
All rights reserved

Crystallization and preliminary X-ray analysis of the *O*-carbamoyltransferase NovN from the novobiocin-biosynthetic cluster of *Streptomyces spheroides*

Crystals of recombinant NovN, an *O*-carbamoyltransferase from *Streptomyces spheroides*, were grown by vapour diffusion. The protein crystallized in two different crystal forms. Crystal form I belonged to space group *C*2 and native data were collected to 2.9 Å resolution in-house. Crystal form II had *I*-centred orthorhombic symmetry and native data were recorded to a resolution of 2.3 Å at a synchrotron. NovN catalyses the final step in the biosynthesis of the aminocoumarin antibiotic novobiocin that targets the essential bacterial enzyme DNA gyrase.

1. Introduction

The aminocoumarin antibiotics are potent inhibitors of the essential bacterial enzyme DNA gyrase (Maxwell, 1997; Maxwell & Lawson, 2003) and thus have attracted considerable interest as potential templates for drug development. The three main compounds novobiocin, clorobiocin and coumermycin A₁ share common structural features, namely an aromatic acyl component (ring *A*), a 3-amino-4,7-dihydroxycoumarin moiety (ring *B*) and an *L*-noviosyl sugar (ring *C*). Clorobiocin and coumermycin A₁ are both decorated at the 3'' position of ring *C* by a 5-methylpyrrole-2-carboxyl moiety, whereas the corresponding modification in novobiocin is a carbamoyl group (Li & Heide, 2006). Previous crystallographic studies on novobiocin complexes of DNA gyrase (Lewis *et al.*, 1996; Holdgate *et al.*, 1997) have shown that the majority of the hydrogen bonds to the target enzyme involve ring *C*, including the carbamoyl group. Indeed, derivatives of novobiocin lacking this moiety were shown to be significantly less potent gyrase inhibitors (Hooper *et al.*, 1982; Flatman *et al.*, 2006). Thus, the attachment of the carbamoyl group, which represents the last step in novobiocin biosynthesis (Kominek & Sebek, 1974; Freel Meyers *et al.*, 2004), deserves closer scrutiny. This reaction is catalysed by the *O*-carbamoyltransferase NovN, which uses carbamoyl phosphate as the co-substrate and is strictly dependent on the presence of ATP (Freel Meyers *et al.*, 2004; Xu *et al.*, 2004). Here, we report the crystallization and preliminary X-ray analysis of NovN from *Streptomyces spheroides* towards elucidating its three-dimensional structure.

2. Materials and methods

2.1. Protein expression, purification and crystallization

The *S. spheroides novN* gene (Swiss-Prot entry Q9L9F4; subunit molecular weight 74 499 Da; 677 amino acids) was amplified by PCR using *S. spheroides* genomic DNA as a template. The amplified DNA was cloned into the vector pET-37b (Novagen) as described by Freel Meyers *et al.* (2004) to give a plasmid encoding the native polypeptide to which the sequence LEHHHHHHHH is appended at the C-terminus (with a total deduced molecular weight of 75 839 Da). This plasmid was transformed into *Escherichia coli* strain BL21 (DE3) (Studier & Moffatt, 1986) and a 10 ml overnight culture of the cells harbouring the pNovN-pET37b construct was used to inoculate a 1 l culture of Luria–Bertani medium containing 50 mg kanamycin. The cells were grown at 310 K to an OD_{600 nm} of around 0.4. Protein expression was induced by the addition of isopropyl β-D-1-thio-

galactopyranoside to a final concentration of 0.1 mM and the culture was left shaking overnight at 288 K. Harvested cells were resuspended in buffer A [25 mM glycine pH 9.0, 500 mM NaCl, 5 mM MgCl₂, 5% (v/v) glycerol, 40 mM imidazole] containing a Complete EDTA-free protease-inhibitor cocktail tablet (Roche) and lysed by three passes through a French press at 6.9 MPa. The cell lysate obtained by centrifugation at 25 000g for 30 min was applied onto a 5 ml Ni²⁺-charged His-Trap Chelating HP column (GE Healthcare) connected to an ÄKTA FPLC system (GE Healthcare). The column was then washed with four column volumes of buffer A and the bound protein was eluted using a linear gradient to 500 mM imidazole in buffer A over five column volumes. The fractions containing NovN (confirmed by SDS-PAGE) were pooled and concentrated using an Amicon Ultra-4 10 kDa cutoff concentrator (Millipore) to a volume of approximately 5 ml. Subsequently, the concentrated protein was applied onto a Superdex-200 HiLoad HP gel-filtration column (GE Healthcare) pre-equilibrated with 25 mM glycine pH 9.0, 200 mM NaCl, 5 mM MgCl₂, 5% (v/v) glycerol and eluted at a flow rate of 1 ml min⁻¹. Fractions containing pure NovN were pooled and concentrated to around 10 mg ml⁻¹ using an Amicon Ultra-4 10 kDa cutoff concentrator (Millipore).

Prior to crystallization, dynamic light scattering (DLS) was used to monitor the solution properties of the protein. For this purpose, approximately 30 µl of sample was centrifuged through a 0.1 µm Ultrafree filter (Millipore) to remove particulate material before introduction into a 12 µl microsampling cell. The latter was then inserted into a Dynapro Titan molecular-sizing instrument at 293 K (Wyatt Technology). A minimum of 15 scattering measurements were taken and the resulting data were analysed using the *DYNAMICS* software package (Wyatt Technology).

Crystallization trials were carried out by vapour diffusion in a sitting-drop format with 96-well Greiner plates using a variety of in-house and commercially available screens (Hampton Research, Molecular Dimensions and Qiagen) at a constant temperature of 291 K. Drops consisted of 1 µl protein solution mixed with 1 µl precipitant solution and the reservoir volume was 50 µl; the protein concentration was approximately 10 mg ml⁻¹. Improved crystals were subsequently obtained by refining the successful conditions in a hanging-drop format using 24-well VDX plates (Hampton Research) over a reservoir volume of 1 ml.

2.2. Cryoprotection and X-ray data collection

Prior to data collection, crystals were soaked for a maximum of 30 s in cryoprotectant, which corresponded to the crystallization solution with the addition of 20% (w/v) xylitol in place of an equivalent volume of water. Crystals were routinely transferred from one solution to another before being ultimately mounted for X-ray data collection using either CryoLoops (Hampton Research) or LithoLoops (Molecular Dimensions).

For in-house data collection, a crystal was flash-cooled to 100 K in a stream of gaseous nitrogen produced by an X-Stream cryocooler (Rigaku-MSK). Diffraction data were collected using a MAR 345 image-plate detector (X-ray Research) mounted on a Rigaku RU-H3RHB rotating-anode X-ray generator (operated at 50 kV and 100 mA) fitted with Osmic confocal optics and a copper target (Cu K α ; $\lambda = 1.542$ Å). For synchrotron data collection, a crystal was flash-cooled by plunging into liquid nitrogen and stored prior to transport to the beamline. The crystal was subsequently transferred to the goniostat on beamline I02 at the Diamond Light Source (UK) and maintained at 100 K with a Cryojet cryocooler (Oxford Instruments). Diffraction data were recorded using an ADSC Quantum 315

CCD detector with the wavelength set to 0.951 Å. All diffraction data were processed using *MOSFLM* (Leslie, 2006) and *SCALA* (Evans, 2006). Preliminary analysis of the data sets was performed using programs from the *CCP4* suite (Collaborative Computational Project, Number 4, 1994).

3. Results and discussion

NovN was overexpressed and purified with an approximate yield of 10 mg protein from 1 l culture and was judged to be greater than 95% pure from SDS-PAGE analysis. DLS analysis gave a monomodal distribution with a relatively low polydispersity of 19%. From these results the molecular size was estimated as 160 kDa, being very close to the value expected for a His-tagged NovN dimer (151.7 kDa).

Preliminary crystals grew within 4 d after set-up from unbuffered 1.75 M (NH₄)₂HPO₄ at 293 K. Improved crystals were subsequently obtained within a range of precipitant concentrations from 1.6 to 2.0 M (NH₄)₂HPO₄ with a variety of additives. Two different crystal forms, denoted I and II, were subsequently characterized.

Data for crystal form I were recorded to 2.9 Å resolution from a single crystal that was grown in the presence of 1 mM ATP (Fig. 1*a*). These data were indexed in the monoclinic space group C2, with unit-cell parameters $a = 161.89$, $b = 108.10$, $c = 96.67$ Å, $\beta = 111.28^\circ$. Estimation of the content of the asymmetric unit based on two His-tagged protomers (75 839 Da each) gave a crystal-packing parameter (V_M) of 2.60 Å³ Da⁻¹, with a corresponding solvent content of 52.7% (Matthews, 1968). Moreover, a self-rotation function calculated using data in the resolution range 10.0–5.0 Å with *MOLREP* (Vagin & Teplyakov, 2000) revealed a noncrystallographic twofold axis perpendicular to the crystallographic twofold axis with a peak height of 24% of the origin peak.

Data for crystal form II were recorded to 2.3 Å resolution from a single crystal that was grown in the presence of 1 mM novobiocin, the product of the NovN reaction (Fig. 1*b*). Indexing was consistent with *I*-centred orthorhombic symmetry, giving unit-cell parameters $a = 107.98$, $b = 111.86$, $c = 166.38$ Å. Estimation of the content of the asymmetric unit based on a single NovN subunit gave a crystal-packing parameter (V_M) of 3.31 Å³ Da⁻¹, with a corresponding solvent content of 62.9% (Matthews, 1968). Data-collection statistics for both crystal forms are given in Table 1.

Interrogation of the *FUGUE* server (<http://www-cryst.bioc.cam.ac.uk/~fugue/prfsearch.html>; Shi *et al.*, 2001) with the NovN sequence

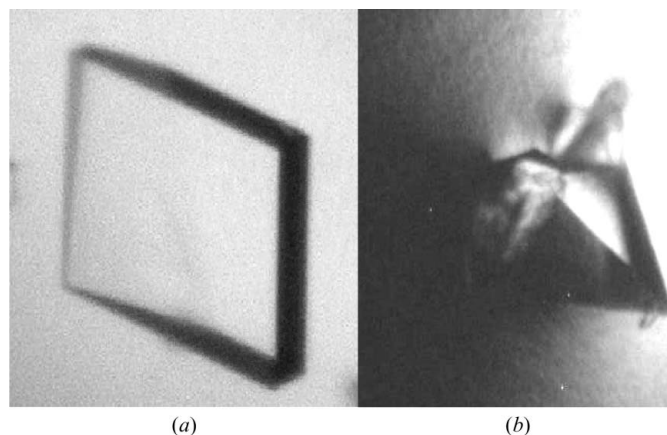


Figure 1
Crystals of *S. sphaeroides* NovN. (a) A single crystal of form I of approximately 300 × 300 × 50 µm in size. (b) Cluster of crystals of form II. The largest single crystal is approximately 300 × 150 × 150 µm in size.

Table 1

Summary of X-ray data for NovN.

Values in parentheses are for the outer resolution shell.

	Form I	Form II
Space group	<i>C2</i>	<i>I222</i> or <i>I212121</i>
Unit-cell parameters (Å, °)	<i>a</i> = 161.89, <i>b</i> = 108.10, <i>c</i> = 96.67, β = 111.28	<i>a</i> = 107.98, <i>b</i> = 111.86, <i>c</i> = 166.38
Wavelength (Å)	1.542	0.951
Resolution range (Å)	26.90–2.90 (3.06–2.90)	47.57–2.29 (2.41–2.29)
Unique reflections	32856 (4875)	44118 (5373)
Completeness (%)	96.1 (98.0)	96.7 (81.8)
Redundancy	1.9 (1.9)	5.8 (3.8)
$R_{\text{merge}}^{\dagger}$	0.100 (0.217)	0.089 (0.414)
$\langle I/\sigma(I) \rangle$	8.0 (3.6)	16.8 (7.4)
Wilson <i>B</i> value (Å ²)	33.7	38.7

$\dagger R_{\text{merge}} = \frac{\sum_{hkl} \sum_i |I_i(hkl) - \langle I(hkl) \rangle|}{\sum_{hkl} \sum_i I_i(hkl)}$, where $I_i(hkl)$ is the *i*th observation of reflection *hkl* and $\langle I(hkl) \rangle$ is the weighted average intensity for all observations *i* of reflection *hkl*.

indicated that there were no suitable templates for molecular replacement in the Protein Data Bank; although two ‘certain’ hits were identified (with *Z* scores of 9.2 and 9.1), their sequence identities with NovN did not exceed 14% over less than half of the NovN sequence. Thus, we will use isomorphous replacement methods to solve the structure of NovN.

IGG and DML would like to thank the BBSRC for financial support through responsive-mode funding (ref. B19400) and the Core Strategic Grant to the John Innes Centre. CLFM and CTW were

funded by NIH grants F32 AI054007 and GM 49338, respectively. R. Chen is acknowledged for isolation of *S. spheroides* genomic DNA. We are also grateful to T. Sorensen for assistance with data collection at the Diamond Light Source.

References

- Collaborative Computational Project, Number 4 (1994). *Acta Cryst.* **D50**, 760–763.
- Evans, P. (2006). *Acta Cryst.* **D62**, 72–82.
- Flatman, R. H., Eustaquio, A., Li, S. M., Heide, L. & Maxwell, A. (2006). *Antimicrob. Agents Chemother.* **50**, 1136–1142.
- Freel Meyers, C. L., Oberthur, M., Xu, H., Heide, L., Kahne, D. & Walsh, C. T. (2004). *Angew. Chem. Int. Ed. Engl.* **43**, 67–70.
- Holdgate, G. A., Tunncliffe, A., Ward, W. H., Weston, S. A., Rosenbrock, G., Barth, P. T., Taylor, I. W., Paupit, R. A. & Timms, D. (1997). *Biochemistry*, **36**, 9663–9673.
- Hooper, D. C., Wolfson, J. S., McHugh, G. L., Winters, M. B. & Swartz, M. N. (1982). *Antimicrob. Agents Chemother.* **22**, 662–671.
- Kominek, L. A. & Sebek, O. K. (1974). *Dev. Ind. Microbiol.* **15**, 60–69.
- Leslie, A. G. W. (2006). *Acta Cryst.* **D62**, 48–57.
- Lewis, R. J., Singh, O. M., Smith, C. V., Skarzynski, T., Maxwell, A., Wonacott, A. J. & Wigley, D. B. (1996). *EMBO J.* **15**, 1412–1420.
- Li, S. M. & Heide, L. (2006). *Planta Med.* **72**, 1093–1099.
- Matthews, B. W. (1968). *J. Mol. Biol.* **33**, 491–497.
- Maxwell, A. (1997). *Trends Microbiol.* **5**, 102–109.
- Maxwell, A. & Lawson, D. M. (2003). *Curr. Top. Med. Chem.* **3**, 283–303.
- Shi, J., Blundell, T. L. & Mizuguchi, K. (2001). *J. Mol. Biol.* **310**, 243–257.
- Studier, F. W. & Moffatt, B. A. (1986). *J. Mol. Biol.* **189**, 113–130.
- Vagin, A. & Teplyakov, A. (2000). *Acta Cryst.* **D56**, 1622–1624.
- Xu, H., Heide, L. & Li, S.-M. (2004). *Chem. Biol.* **11**, 655–662.